E7-2006-75

Yu. E. Penionzhkevich[1], R. A. Astabatyan[1], N. A. Demekhina[2],
G. G. Gulbekian[1], R. Kalpakchieva[1], A. A. Kulko[1],
S. M. Lukyanov[1], E. R. Markaryan[1], V. A. Maslov[1],
Yu. A. Muzychka[1], Yu. Ts. Oganessian[1], R. V. Revenko[1],
N. K. Skobelev[1], Yu. G. Sobolev[1], D. A. Testov[1],
T. Zholdybaev[3]

EXCITATION FUNCTIONS OF FUSION REACTIONS AND NEUTRON TRANSFER IN THE INTERACTION OF ^{6}He WITH ^{197}Au AND ^{206}Pb

Submitted to «European Physical Journal A»

[1]Flerov Laboratory of Nuclear Reactions, Joint Institute for Nuclear Research, Dubna, Russia
[2] Yerevan Physics Institute, Yerevan, Armenia
[3] Institute of Nuclear Physics, Almaty-82, Kazakhstan

Пенионжкевич Ю. Э. и др. E7-2006-75

Функции возбуждения реакций слияния и передачи нейтронов
при взаимодействии ионов ^{6}He с ^{197}Au и ^{206}Pb

Экспериментально измерены функции возбуждения для реакций слияния с последующим испарением нейтронов $^{197}\mathrm{Au}(^{6}\mathrm{He}, xn)^{203-xn}\mathrm{Tl}$, где $x = 2{-}7$, и $^{206}\mathrm{Pb}(^{6}\mathrm{He}, 2n)^{210}\mathrm{Po}$, а также для каналов передачи на ^{197}Au с образованием изотопов ^{196}Au и ^{198}Au. Мишени из ^{197}Au и ^{206}Pb облучались ^{6}He на ускорительном комплексе радиоактивных пучков DRIBs ОИЯИ. Интенсивность пучка ^{6}He составляла $2 \cdot 10^{7}$ с$^{-1}$, максимальная энергия около 10 МэВ/А. Стопки мишеней облучались на прямом пучке или на пучке после анализа в магнитном спектрометре МСП-144. Идентификация продуктов проводилась по характеристикам их γ- или α-распадов. Наблюдалось необычно высокое сечение образования изотопа ^{198}Au при энергиях ниже кулоновского барьера. Рассмотрены возможные механизмы образования и распада продуктов реакций передачи нуклонов. Имеет место значительное увеличение сечения канала реакции слияния с испарением двух нейтронов в подбарьерной области энергий по сравнению с расчетами по статистической модели. Проведенный анализ экспериментальных данных в рамках статистической модели распада возбужденных ядер с учетом последовательного слияния ядер ^{6}He показал хорошее согласие экспериментальных и расчетных значений сечения для подбарьерного слияния ядер в реакции $^{206}\mathrm{Pb} + {}^{6}\mathrm{He}$.

Работа выполнена в Лаборатории ядерных реакций им. Г. Н. Флерова ОИЯИ.

Препринт Объединенного института ядерных исследований. Дубна, 2006

Penionzhkevich Yu. E. et al. E7-2006-75

Excitation Functions of Fusion Reactions and Neutron Transfer
in the Interaction of ^{6}He with ^{197}Au and ^{206}Pb

Excitation functions for evaporation residues in the reactions $^{197}\mathrm{Au}(^{6}\mathrm{He}, xn)^{203-xn}\mathrm{Tl}$, where $x = 2{-}7$, and $^{206}\mathrm{Pb}(^{6}\mathrm{He}, 2n)^{210}\mathrm{Po}$, as well as for neutron transfer reactions for the production of ^{196}Au and ^{198}Au in the interaction of ^{6}He with ^{197}Au were measured. ^{6}He beam was obtained from the accelerator complex for radioactive beams DRIBs (JINR). The energy of the incident beam was about 10 MeV/A and the intensity reached 2×10^{7} pps. The stacked foil technique was used directly in the beam extracted from the cyclotron or in the focal plane of the magnetic spectrometer MSP-144. The identification of the reaction products was done by their radioactive γ or α decay. Unusually large cross section was observed below the Coulomb barrier for the production of ^{198}Au in the interaction of ^{6}He with ^{197}Au. Possible mechanisms of formation and decay of transfer reaction products are discussed. An increase in the cross section was observed for the fusion reaction with the evaporation of two neutrons compared to statistical model calculations. The analysis of the data in the framework of the statistical model for the decay of excited nuclei, which took into account the sequential fusion of ^{6}He has shown good agreement between the experimental and the calculated values of the cross sections for the case of sub-Coulomb-barrier fusion in the $^{206}\mathrm{Pb} + {}^{6}\mathrm{He}$ reaction.

The investigation has been performed at the Flerov Laboratory of Nuclear Reactions, JINR.

Preprint of the Joint Institute for Nuclear Research. Dubna, 2006

1. INTRODUCTION

The investigations of the interaction of ^{6}He with other nuclei make it possible to obtain information on the structure of this exotic nucleus. In spite of the almost 10-years history of these and other studies with a variety of exotic nuclei, there is still controversy in the interpretation of the data obtained. Of interest from experimental and theoretical point of view continue to be reactions induced by neutron halo nuclei. Especially much attention is paid to ^{6}He-induced reactions leading to the formation of compound nuclei, which then can decay by the evaporation of neutrons or fission. The first experimental paper [1] on the subject was dedicated to the study of fission of the compound nucleus ^{215}At, formed in the bombardment of a ^{209}Bi target with ^{6}He ions. A significant enhancement was observed in the cross section, especially in the sub-Coulomb barrier energy region, compared to what was expected according to the statistical model. Such an enhancement was earlier predicted in a series of theoretical papers [2,3]. In particular, an increase of the probability of penetrating (tunneling) through the potential barrier due to its extended neutron distribution, compared to that in ordinary nuclei close to the line of stability, was predicted for ^{11}Li. Such distributions, as has been shown in ref. [4] may bring forth a coupling of the collective degrees of freedom and, respectively, an increase of the reaction cross section, especially in the sub-barrier region.

The extended distribution of nuclear matter is characteristic for light neutron-rich nuclei, in which the presence of valence neutrons can lead to the formation of a neutron halo. ^{6}He and ^{11}Li are among the nuclei with such a structure. Different reaction mechanisms can manifest themselves in the interaction. Among them are the exchanges of one or several nucleons between the target and projectile, inelastic scattering, etc. Additionally, the weak binding of the halo neutrons leads to an increase in the probability of the breakup of the nuclei. This may be accompanied by the consequent capture of the residual core by the target nucleus or by the transfer of nucleons without any further interaction between the nuclei – this exit channel can be referred to as stripping. The variety of possible processes makes it difficult to analyze the experimental data and requires the consideration of all possible reaction channels.

Soon after the first experimental paper on the fusion-fission reaction induced by ^{6}He [1], a series of experiments was undertaken, whose aim was to determine the probability of fusion of ^{6}He with other nuclei close to the Coulomb barrier. For instance, in [5] investigated the same reaction, ^{209}Bi +

^{6}He, as was used in [1]. The excitation function for the decay of the compound nucleus by emission of three neutrons was measured and the comparison with the statistical model for the formation and decay of the compound nucleus confirmed that an enhancement of sub-barrier fusion of ^{6}He nuclei takes place. The next measurement of the excitation function for the fission channel in the ^{6}He + ^{238}U reaction [6] also allowed to draw the conclusion that the probability of fusion-fission, when using a ^{6}He beam at Coulomb barrier energies, is strongly enhanced. However, a later experiment of the same group involving the measurement of the fission fragments in coincidence with α-particles, produced after the breakup of ^{6}He, has shown that sub-barrier fusion-fission for this reaction can easily be explained in terms of the fission of the uranium target after the transfer of one or two neutrons. This circumstance led to a new paper [7] of the same authors [6], in which they insisted that no enhancement of the fusion of ^{6}He was present in the mentioned reaction. There are a few more papers reporting on fusion reactions with ^{6}He [8,9]. However, these measurements require the inclusion of more information on the different exit channels and higher statistics in order to be considerably more reliable.

The existence of such controversial data is evidence of the difficulties, which have to be overcome in experiments with radioactive ion beams. One such problem, in the first place, is the low intensity of the secondary beams. This makes measurements in the region of the Coulomb barrier extremely time consuming, if high statistics is to be obtained. Secondly, in order to study the excitation functions in a broad energy range (5-70 MeV/A), it is necessary to decrease the beam energy using degraders, which in turn deteriorates the beam energy dispersion. Finally, at the relatively low beam intensity, it is desirable to use detector arrays of high efficiency, located at forward angles with respect to the beam direction.

It is necessary to note that such conditions can be provided only at facilities based on the ISOL-method. Such facilities in addition to DRIBs are SPIRAL1 in France and the accelerator at Louvain-la-Neuve (Belgium).

All this we took into account when preparing the experiments described below. The launching of the accelerator complex for radioactive beams DRIBs [10] at FLNR (JINR) in the end of 2004 made it possible to produce ^{6}He beams with an intensity of up to $5 \cdot 10^{6}$ pps in a wide range of energies (3-10 MeV/A), the energy resolution being not worse than 1 %. The results of the first experiment aimed to study the interaction of ^{6}He with ^{197}Au and ^{206}Pb have been already published in [11]. In the present paper we report on new measurements of the excitation functions of product nuclei from the reactions ^{197}Au(^{6}He,xn)$^{203\text{-}xn}$Tl, where x=2-7, and

^{206}Pb(^{6}He,2n)^{210}Po, as well as for the transfer reactions on a ^{197}Au target with the formation of the ^{196}Au and ^{198}Au isotopes, with a beam dose about a factor of 10 higher and, in addition, at energies considerably lower than the Coulomb barrier of the reactions.

2. EXPERIMENTAL METHOD

In the experiments, a beam of accelerated ^{6}He ions with an energy of up to about 10 MeV/A was used. It was provided by the DRIBs complex at FLNR, JINR [10]. This complex is a tandem including the FLNR cyclotrons U400M and U400 (Fig. 1). The ^{6}He nuclei were produced in a thick beryllium or carbon target bombarded with a ^{7}Li beam accelerated to 35 MeV/A (its intensity being 1-1.5 eμA) at the U400M accelerator and diffused into the ECR-source chamber from a porous carbon catcher (heated up to 1600° C). After ionization of the ^{6}He atoms in the ion source, the single-charged ^{6}He ions were transported to the second accelerator U400, where they were further accelerated to an energy of about 10 MeV/A with intensity up to $2 \cdot 10^{7}$ pps.

The $^{6}He^{+2}$ beam was extracted from the U400 cyclotron by a thin aluminum stripping foil. The optimization and transport of the $^{6}He^{+2}$-ion beam made it possible, without applying any additional collimation, to have a (7 x 7)-mm beam spot on the physical targets.

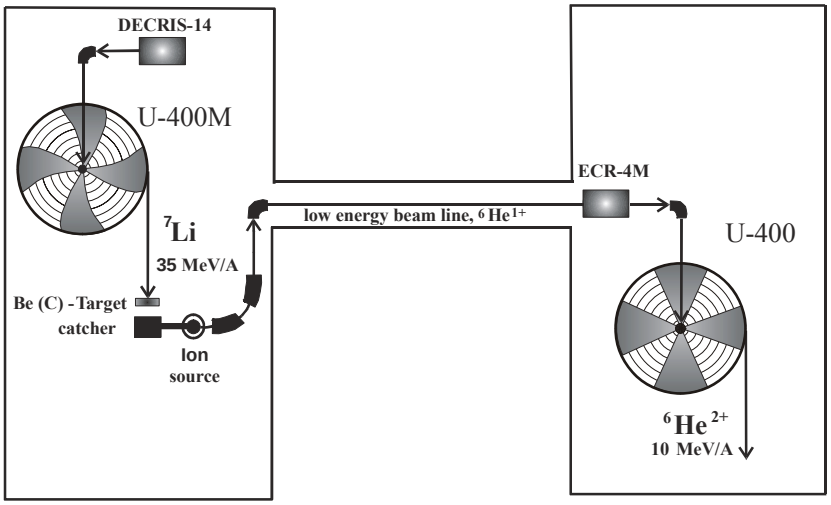

Fig. 1. Schematic layout of the complex DRIBs for producing the radioactive ^{6}He beam.

For the beam diagnostics of the low-energy ^{6}He ions, scintillation detectors were placed [12] in the beam-transport line, whereas immediately in front of the physical setup the parameters of the beam (intensity and size) were measured with a specially designed multi-wire proportional chamber [13]. The energy of the beam was measured with the MSP-144 magnetic spectrometer [14] or with a semiconductor detector placed at 0° relative to the beam direction.

A total of four runs were carried out (see Table 1). The energy of the beam extracted from the cyclotron is given in the second column. The energies of the beam on entering the first target (column 4) and their energy spread (column 5) were directly measured, as will be described below. The experiments were aimed at studying the interaction of ^{6}He with the target nuclei ^{197}Au and ^{206}Pb. The excitation functions of the fusion reactions with the consequent evaporation of 2 to 7 neutrons from the compound nuclei and of transfer reactions were measured.

Table 1. Initial ^{6}He-beam energy (E_{ini}), energy at the first physical target ($E_{1st\text{-}tar}$), energy spread (FWHM) and beam intensity on target.

Run №	E_{ini}(^{6}He) [MeV]	FWHM [MeV]	$E_{1st\text{-}tar}$(^{6}He) [MeV]	FWHM [MeV]	Intensity on target [pps]	Ref.
1.	60.3	±0.4	60.3 (Au) 21.8 (Pb)	±0.4	$5\cdot10^{6}$	[11]
2.	60.9	±0.4	43.3	±0.6	$2\cdot10^{6}$	**
3.	61.2	±0.8	25.5 (Pb) 10.3 (Au)	±1.1 ±2.3	$\sim10^{7}$	**
4.	61.9	±0.7	23.3 (Au)	±0.25	$5\cdot10^{5}$	**

** - present work

In all runs, the measurement of the yields of the fusion reaction evaporation residues and of the transfer reactions was performed by the activation method.

The details of Run 1 are presented in ref. [11]. Here we shall mention them only briefly. Two stacks of foils were placed in the reaction chamber of the magnetic spectrometer MSP-144 one after the other: first – a stack consisting of one 50-μm and twelve 13-μm thick gold foils, and further downstream – a second stack of six ^{206}Pb targets, 600-700 μg/cm^2 each (Fig. 2). In order to tune the ^{6}He beam and to measure its intensity and spatial distribution, the multi-wire proportional chamber for beam diagnostics was

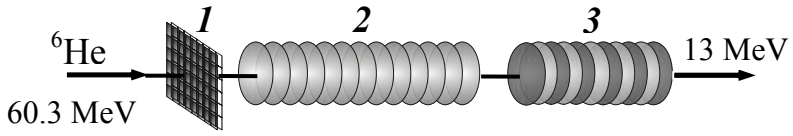

Fig. 2. Schematic layout of the activation experiments using the ^{6}He beam (Run 1):
1 – multi-wire proportional chamber, specially designed for beam diagnostics; *2* – stack of gold foils, and *3* – stack of six thin ^{206}Pb-targets. The incident and final energy of the beam are also shown.

placed in front of the stacks. After passing through the two stacks, the beam entered the magnetic spectrometer MSP-144, which gave a precise measurement of the residual energy of the beam. The ^{6}He energy and the energy loss in each layer of the stacks were calculated with the LISE code [15] and the calculated residual energy was compared to the value measured by the magnetic spectrometer. In this way, in spite of the rather large energy dispersion of the beam after the last target in the stack (±2 MeV), the absolute value of the energy at each target was determined with good accuracy (better than 1 MeV).

In Run 2 only a stack of fifteen ^{197}Au (seven 13-μm, four 5-μm and four 4-μm) targets was irradiated. Different absorbers were used to decrease the initial energy of the beam down to 43.3 MeV. The energy incident on each successive target was determined separately by multiple measurements using a semiconductor monitor detector placed at 0° relative to the beam. The measured FWHM and the energy loss in each target were used to define the uncertainty in the energy values for each cross section point. The energy values refer to the middle of the targets.

In Run 3, the initial energy was lowered to 25.5 MeV by means of two foils: a gold one, which served also as a target for the excitation function on ^{197}Au, and an Al one. A stack of seven thin ^{206}Pb targets was used. After it, two 5-μm ^{197}Au targets were placed in order to measure the transfer reactions deeply below ($E \leq 10$ MeV) the Coulomb barrier of the reaction ($E \approx 20.9$ MeV). As in Run 2, before the stack was finally assembled and irradiated, the energy of the beam entering each successive target was measured by the monitor detector at 0°. During the irradiation, the monitor was kept in the beam to control its stability.

In Run 4, the stringent requirements, concerning the stability of the beam and the necessity to reduce as much as possible the energy spread of the beam falling on the ^{197}Au targets at very low energies, were met by

placing the stack of gold foils at the focal plane of the magnetic spectrometer MSP-144 [14]. The layout of the experimental setup is shown in Fig. 3. In this case, the energy of the beam stringent on the stack was $E \pm \delta E$, where δE was determined by the extension of the target along the focal plane (18 mm), which corresponded to a value of ±250 keV. The ^{197}Au stack contained 7 foils each 6.6 μm thick. The initial energy of the ^{6}He beam was reduced to 23.3 MeV. The energy and its spatial distribution were measured by varying the magnetic field in the magnetic spectrometer: two independent detection arrays were used – the MSP focal plane detector and two PIN detectors placed at two different positions on the focal plane. After this, the ^{197}Au stack was placed at the position of the maximum beam intensity. The beam dose on the stack was measured by a scintillation counter behind it. On both sides, other counters were placed for additional control of the beam quality. The long-term high stability (about 10^{-5}) of the magnetic field of the spectrometer allowed defining the final energy spread for each calculated cross section point mainly by the energy loss in each target.

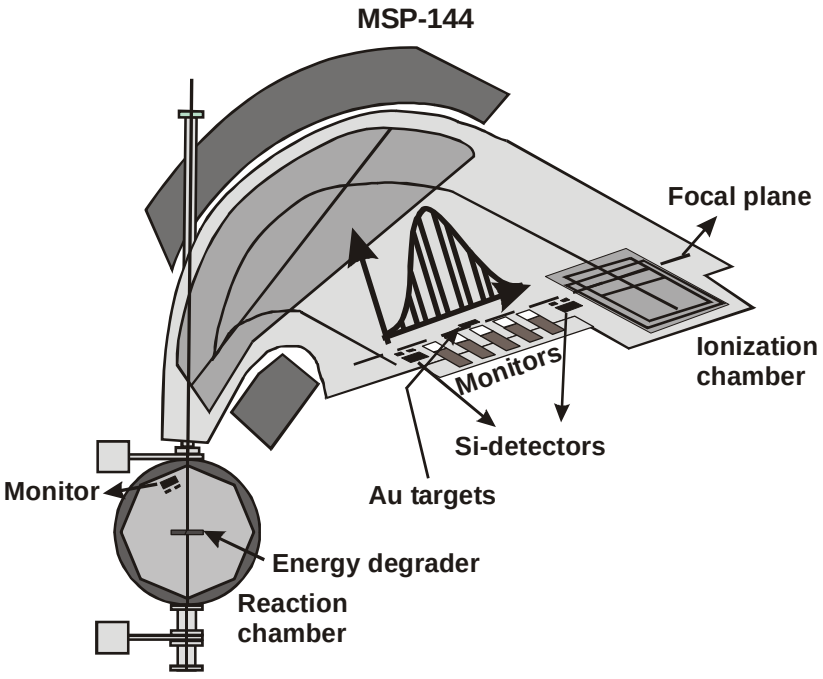

Fig. 3. Schematic layout of the activation experiments using the MSP-144 magnetic spectrometer.

After the irradiation the γ-activity induced in the gold foils was measured off-line using four energy and efficiency calibrated HPGe detectors (the efficiency was about 4-5 % for $E_\gamma = 662$ keV) of high-energy resolution (1.2 keV for the γ-transition at 1332 keV). For the analysis of the γ-spectra, the program DEIMOS 32 [16] was used. Peaks in the γ-spectra (see, for example, Fig. 4) could be identified as belonging to the Tl isotopes, which are the decay products of the compound nucleus ^{203}Tl after the evaporation of 2-7 neutrons.

In addition to the Tl isotopes, the production of the isotopes ^{194}Au, ^{196}Au and ^{198}Au could be identified in the spectra measured for the gold targets by means of the γ-transitions following their decay.

Table 2 contains the decay date – energies, half-lives and absolute yields of the most intensive γ-transitions in the corresponding fusion reaction decay products, which have been used for their identification.

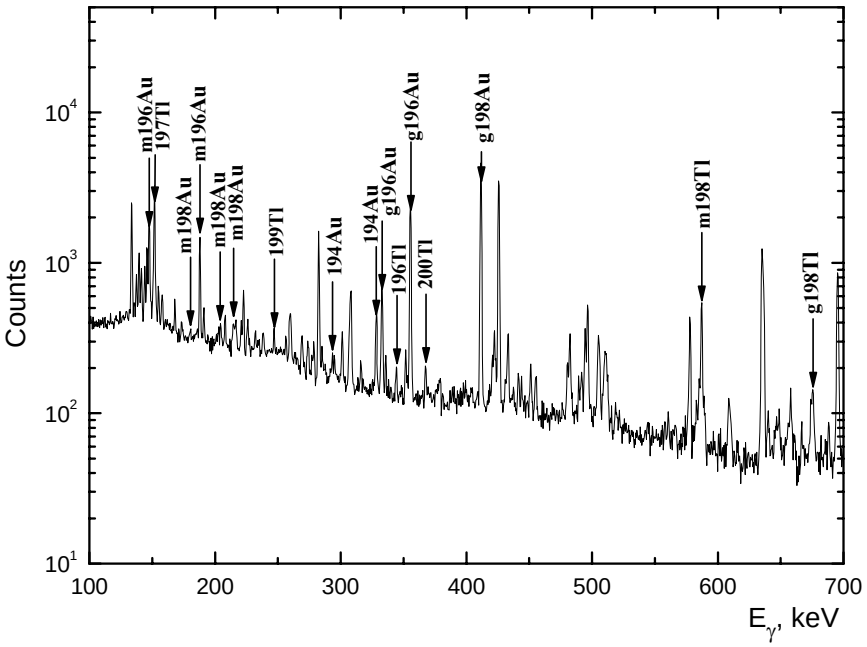

Fig. 4. Fragment of the gamma spectrum, obtained from measurement of the induced activity in the 16 μm Au-foil irradiated with the ^{6}He beam at ~60 MeV. The γ-transition identification is shown next to the peaks. The formation of the ground and isomeric states is denoted by g and m, respectively.

Table 2. Characteristics of the decay products of the compound nucleus ^{203}Tl and of the ^{194}Au, ^{195}Au, ^{196}Au, ^{198}Au and ^{199}Au isotopes [17].

Decay product	Half-life $T_{1/2}$	$E\gamma$, keV	I %
^{201}Tl	72.91 h	167.4	10
^{200}Tl	26.1 h	367.9 579.3 1205.7	87 13.8 29.9
^{199}Tl	7.42 h	247.3	9.3
^{198}Tl	5.3 h	675.9	11
^{198m}Tl	1.87 h	587.2	52
^{197}Tl	2.84 h	152.2	7.3
^{196}Tl	1.84 h	344.9	2
^{196m}Tl	1.41 h	505.2 695.6	6 41
^{194}Au	38.02 h	293.5 328.4	10.4 61
^{195}Au	186.09 d	98.8	10.9
^{196g}Au	6.183 d	333 355.7	22.9 86.9
^{196m2}Au	9.6 h	147.7 188.2	43 37.4
^{198g}Au	2.696 d	411.8	95.5
^{198m}Au	2.3 d	180.3 204.1 214.9	50 40.8 77
^{199}Au	3.139 d	158.4 208.2	40 8.7

The cross sections for the formation of the reaction products were calculated taking into account the relevant beam dose and time factors, the target thickness, the decay characteristics of the identified isotopes by the following formula [18]:

$$\sigma = \frac{S\lambda}{d\phi I\varepsilon(1-e^{-\lambda t_1})e^{-\lambda t_2}(1-e^{-\lambda t_3})}, \qquad (1)$$

where S is the number of counts in the photo-peak for the time of γ-spectrum measurement t_3, λ – the decay constant of a given isotope, t_2 – the time elapsed between the end of irradiation and the start of the measurement, t_1 – the time of irradiation, d – the target thickness in atoms/cm^2, ϕ – the beam intensity in unit time, I – the absolute intensity of the given γ-transition, and ε – the γ-detector efficiency for the given γ-line. In the case, when an isotope could be produced in its isomeric and ground state, then the independent production cross section of the ground state was calculated using the relation [19]:

$$\sigma_d = \frac{\left(\frac{S}{d\phi I\varepsilon} - k_{br}\sigma_p A\right)\lambda_d}{(1-e^{-\lambda_d t_1})e^{-\lambda_d t_2}(1-e^{-\lambda_d t_3})};$$

$$A = \frac{\lambda_p\lambda_d}{\lambda_d-\lambda_p}\left[\frac{(1-e^{-\lambda_p t_1})}{\lambda_p^2}e^{-\lambda_p t_2}(1-e^{-\lambda_p t_3}) - \frac{(1-e^{-\lambda_d t_1})}{\lambda_d^2}e^{-\lambda_d t_2}(1-e^{-\lambda_d t_3})\right], \qquad (2)$$

where σ_p, σ_d denote the cross sections of the considered parent (isomeric) and daughter (ground) state, respectively, λ_p, λ_d – their decay constants, k_{br} – the branching coefficient for the given decay scheme. The statistical errors for the cross section values have been obtained as mean square of the errors of the extracted peak area, the subtracted background, as well as the detector's efficiency errors. The energy dispersion at each cross section point represents the mean square of the measured energy spread and the energy loss of the ^{6}He beam in each foil, whereas the each energy value relates to the middle of the respective target.

The ^{206}Pb stack was measured using an α-spectrometer and the excitation function for the formation of the compound nucleus ^{212}Po and its decay by emission of two neutrons, ^{206}Pb(^{6}He,2n)^{210}Po, was obtained in the beam-energy range 10-25.5 MeV (the Coulomb barrier for the given reaction is 21.5 MeV). The ^{210}Po isotope was identified by the α-particle energy

(E_α = 5.3 MeV) and its half-life ($T_{1/2}$ = 138 d). The energy resolution of the α-spectrometer amounted to about 50 keV, and the total efficiency of registration of the α-particles was about 50 %.

3. RESULTS AND ANALYSIS

On the basis of the measured yields of the isotopes, formed after the evaporation from the compound nucleus ^{203}Tl of 2 to 7 neutrons, taking into account the ^{6}He beam intensity and the target thickness, we could determine the cross sections for the formation of the different isotopes and their dependence on the bombarding energy (the excitation functions). The same procedure was applied for ^{210}Po, which was formed in the ^{206}Pb(^{6}He,2n)^{210}Po reaction.

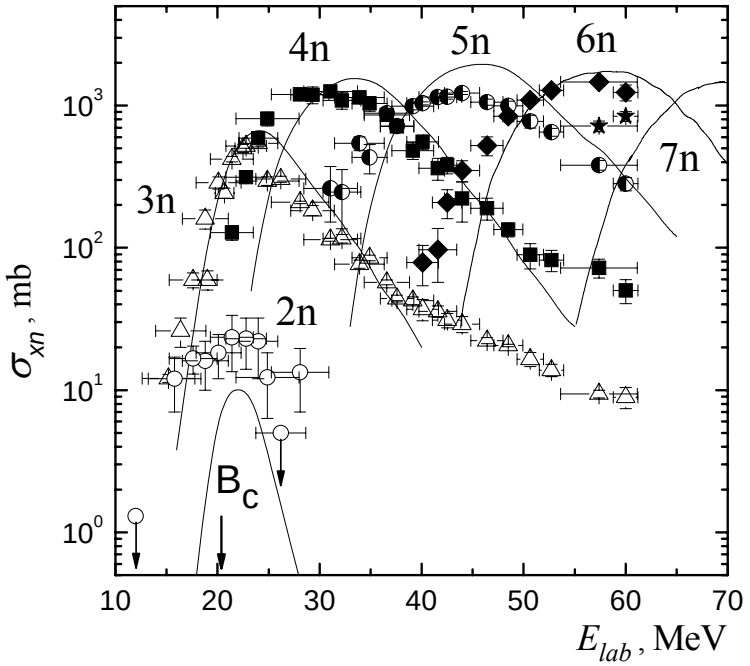

Fig. 5. Experimental excitation functions for the ^{197}Au + ^{6}He → $^{203\text{-}xn}$Tl reaction, where x = 2-7. The symbols denote: – – 2n, Δ – 3n, ! – 4n, 6– 5n, Λ – 6n, ξ – 7n evaporation channels; the curves – calculations with the "ALICE-MP" code [20,21] using the following parameters for the interaction potential: r_0 = 1.29 fm, V = -67 MeV and d = 0.4 fm [21]. B_c is the Coulomb barrier for the ^{6}He + ^{197}Au reaction.

The excitation functions measured for the reaction channels ^{6}He + ^{197}Au $\rightarrow$ $^{203-x}$Tl, where x=2-7 are shown in Fig. 5. The analysis of the obtained data was performed using the code "ALICE-MP" [20]. The values of the parameters used were taken from analyses of experimental data on the cross sections of evaporation reaction channels induced by heavy ions in the range of medium and heavy nuclei [21]. The solid curves in Fig. 5 represent the results of the calculations in the framework of the statistical model of decay of compound nuclei. It can be seen that the experimental and calculated cross sections at the maxima are in agreement what concerns the evaporation of 3-7 neutrons. Except that at somewhat higher energies, a retarded decrease in the cross section is present. Such high-energy "tails" have been formerly observed in α-particle induced reactions and have been explained as due to pre-equilibrium emission [22].

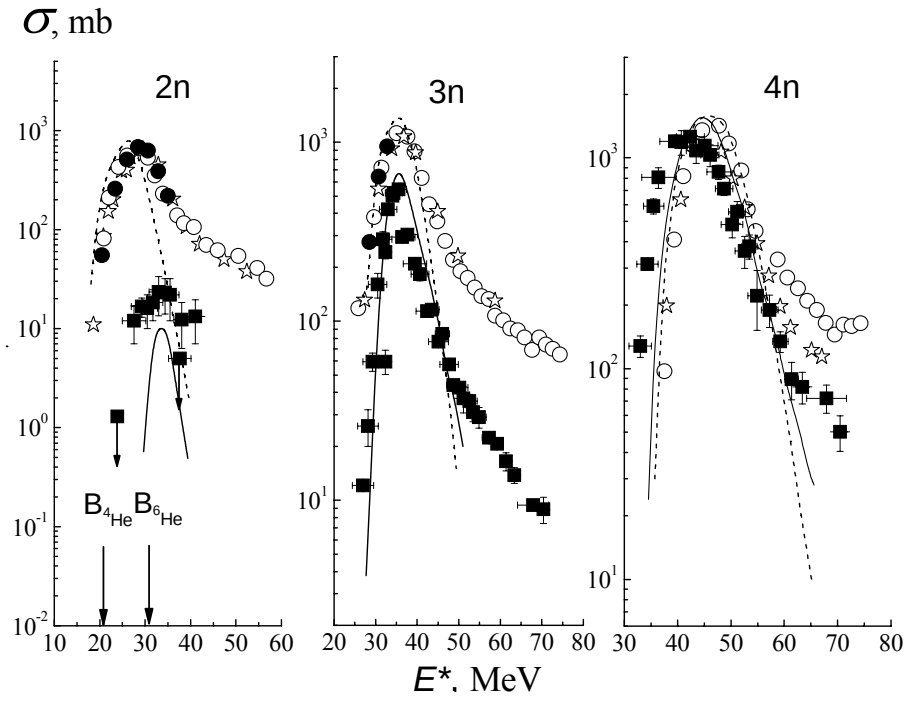

Fig. 6. Cross sections for different evaporation residues, obtained in the ^{197}Au(^{6}He,xn) reaction (!-present work), compared with results from ^{197}Au(^{4}He,xn) [23 and references therein].

Direct analogy in the behavior of the excitation functions of reactions with ^{6}He and ^{4}He can be demonstrated, if we compare the excitation functions of the two reactions ^{197}Au(^{6}He,xn) and ^{197}Au(^{4}He,xn) [23], as a function of excitation energy. Such a comparison is made in Fig. 6 for the evaporation channels with x = 2, 3 and 4. As shown in the figure, at energies above the maximum of their excitation functions, the experimental cross sections for the case of the incident ^{6}He fall off faster than in the case of ^{4}He. From the comparison of these spectra, a conclusion can be drawn that in the process of formation of a compound nucleus, the α-particle core in ^{6}He behaves as a free ^{4}He nucleus. This could be expected due to the weak binding of the valence neutrons with the α-particle. Obviously, in the 3n-evaporation channel one neutron is emitted from the α-particle core, while the other two are "provided" by the valence neutrons of ^{6}He. Because of this, it can be assumed that the 3n-channel in the case of the ^{6}He-induced reaction is an analog of the 1n-channel in the reaction with the ^{4}He beam. In the 4n-channel, the pre-equilibrium neutrons can be 1 or 2.

Contrary to the excitation functions for x = 3-7, the cross sections for the 2n-exit channel (the nucleus ^{201}Tl is formed) are significantly higher than the values, calculated using the one-dimensional barrier between the interacting nuclei [20]. This may be connected with the fact that the reaction with total absorption of ^{6}He by the ^{197}Au target nucleus has a large positive *Q*-value, equal to +12.2 MeV. Thus, the position of the maximum of the excitation function for the evaporation of two neutrons is deeply below the barrier. Therefore, the noticeable difference between the calculated and experimental cross sections must be the result of sub-barrier enhancement.

We have observed quite a similar situation in the case of the interaction of ^{6}He with ^{206}Pb. The difference between the two reactions lies in the fact that in the ^{6}He + ^{206}Pb case, the *Q*-value is equal to +4.2 MeV. This, in turn, makes the 2n-channel less "sub-barrier", and, consequently, leads to somewhat larger cross section values.

The difference between experiment and calculations is particularly well seen in Fig. 7, where the excitation function for the ^{206}Pb(^{6}He,2n)^{210}Po reaction is shown. The cross section for this reaction at the maximum, according to the statistical model calculations (the dashed line), should be small, because the maximum is situated at energies below the Coulomb barrier. However, as can be seen from the presented data, even at energies 7 MeV below the Coulomb barrier for the ^{206}Pb + ^{6}He reaction, the cross section for formation of ^{210}Po, i.e. for the evaporation from the compound nucleus of two neutrons, is rather large and amounts to 10 mb. Thus, due to the observation of the reaction with the evaporation of two neutrons we could

draw the conclusion that a considerable enhancement of the cross section for the fusion of ^{6}He with the ^{197}Au and ^{206}Pb nuclei exists at energies close to the barrier. In the same figure, the results of the calculations for the two-step fusion process are also presented [24]. In this model, it is assumed that a consecutive transfer of neutrons from the ^{6}He nucleus to the target nucleus takes place. At this, the excitation energy of the nuclear system increases by $E_{cm}+Q_{gg}$, a value that is quite higher than the Coulomb barrier and leads to the tunneling, at the latest stage, of the particle through the barrier.

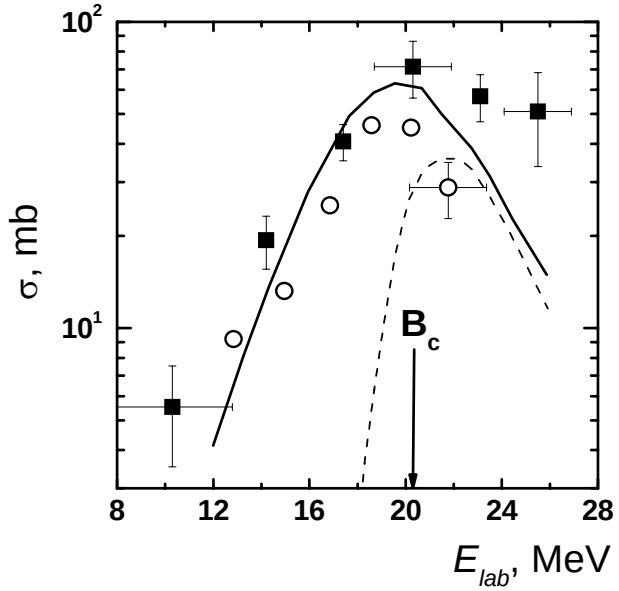

Fig. 7. Excitation function measured for the ^{206}Pb(^{6}He,2n)^{210}Po reaction.
–, ! - denote experimental cross sections for the formation of ^{210}Po (open and black symbols are results from Run 1 and Run 3, respectively), dashed line – calculations within the framework of the statistical model, solid line – calculations using the two-step fusion model [24], taking into account the beam energy spread. B_c is the Coulomb barrier.

The agreement between the experimental reaction cross sections for the ^{206}Pb(^{6}He,2n)^{210}Po reaction with the calculated ones can be considered as evidence that the sequential fusion process for weakly bound nuclei seems to be the main process, which influences the fusion probability of ^{6}He with ^{206}Pb and leads to the increase in the reaction cross section at energies far below the barrier.

The measured excitation functions for the formation of the gold isotopes ^{194}Au, ^{196}Au and ^{198}Au in their ground states in the ^{6}He + ^{197}Au reaction are shown in Fig. 8. We tried to explain the behavior of the cross sections from the point of view of kinematics and reaction dynamics.

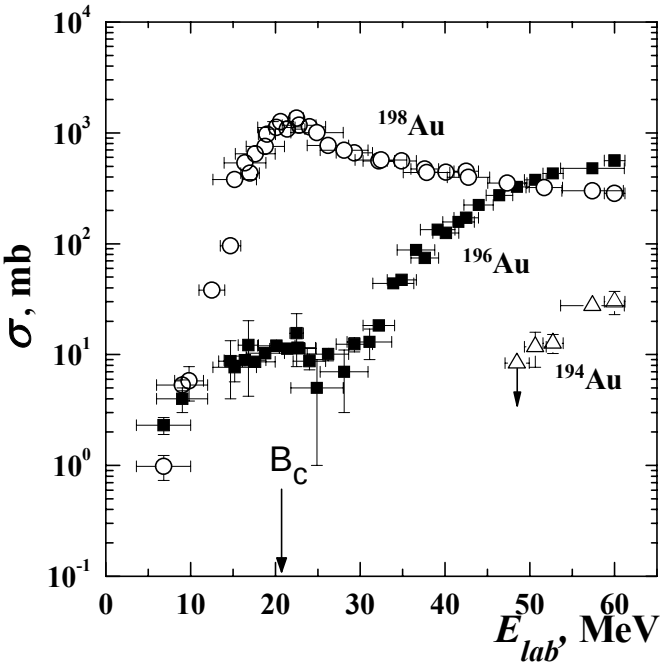

Fig. 8. Experimental excitation functions for the formation of the isotopes 8- ^{194}Au, !- ^{196}Au and –- ^{198}Au in the ^{197}Au + ^{6}He reaction.

Before that the following remark should be made. The contribution of transfer of charged particles and complete fusion to the formation of these isotopes is negligibly small. As shown by calculations within the statistical model, this probability amounts to less than 0.01 for the used energy range. As a result, mainly neutron transfer contributes to the formation of the gold isotopes.

Thus, the simplest ways in which target-like isotopes might be formed in the given reaction are: the isotopes ^{196}Au and ^{194}Au result after the removal of one and three neutrons from ^{197}Au, respectively, whereas ^{198}Au is formed after the pick-up by ^{197}Au of one neutron from ^{6}He. The isotope ^{199}Au was not observed, but we shall nevertheless make some remarks on it in connection with the formation of the lighter isotopes.

It should be noted that the xn-separation energies in the target-like residues control the survivability of the given reaction products. We shall use the prescription of ref. [25] in order to estimate the minimum and maximum excitation energy in the heavy nucleus, necessary to evaporate x-neutrons:

$$E^*_{\min} = \sum_{n=1}^{x} B_n + 1.7x \ , \qquad (3)$$

$$E^*_{\max} = \sum_{n=1}^{x+1} B_n + 1.7(x+1) \ , \qquad (4)$$

where B_n is the binding energy of the n^{th} neutron (the values of nuclear masses and separation energies of one, two, etc. neutrons are taken from [26]).

The isotope ^{199}Au. The production of ^{199}Au involves a large reaction Q-value (Q_{gg} = +13.12 MeV), which means that there is kinematical mismatch, leading to low cross section. In fact, in our experiments, only an upper limit for the formation of the ^{199}Au isotope was determined. This gives evidence for the low probability of populating the ground state of this nucleus when ^{6}He interacts with ^{197}Au. Indeed, the transfer of two neutrons in this case takes place to particle-unbound states in ^{199}Au, which means that it immediately emits one (transition to ^{198}Au) or more neutrons (transition to lighter Au isotopes).

The isotope ^{198}Au. As can be seen in Fig. 8, close to the barrier, the probability of producing the ^{198}Au isotope is rather large ($\sigma \sim 1.2$ b). At first consideration, this may be taken as direct evidence of large pure 1n-transfer cross section. That would mean that the isotope ^{198}Au is formed by 1n-transfer to the ^{197}Au target, followed by γ-transitions to its ground state. In fact, the reaction Q-value for the process of "^{6}He 1n-stripping" (or pick-up of one neutron by the ^{197}Au target nucleus) is Q_{gg} = 4.65 MeV, while the separation energy of one neutron from ^{198}Au is 6.51 MeV; therefore, there is some probability for radiation transition to the ground state.

Another way of producing ^{198}Au is also possible, viz. in the transfer of two neutrons to the ^{197}Au target nucleus and de-excitation of the recoiling target-like nucleus ^{199}Au through the emission of one neutron. As mentioned above, the production of ^{199}Au involves a value Q_{gg} = 13.12 MeV and, since B_{1n} = 7.58 MeV, the channel of 1n-evaporation is open to produce ^{198}Au.

Obviously, the contribution of these two paths to ^{198}Au may vary at different incident energies.

At the same time, the probability of 3n-transfer to ^{197}Au with subsequent evaporation of two neutrons is small. This follows from the low possibility to pick up one neutron from ^{4}He [23].

As it is known, ^{197}Au has a large cross section for pick-up of thermal neutrons. In order to study the effect of background neutrons on the results, we placed a thick Au foil next to our stack. The γ-spectra measurements of this target showed that in our case the contribution of background-neutron-capture to produce ^{198}Au was insignificant.

As shown in Fig. 8, the cross section for the transfer of one neutron to ^{197}Au falls down to about 1 mb at ~7 MeV. The rather fast drop of the cross section for the formation of ^{198}Au in the sub-barrier region can be considered also as due to the turning point of the entrance channel getting further when going away from the barrier and to the exponential dependence of the transfer form factor on the turning point radius.

The observed effect in our experimental data on ^{198}Au can be compared to the situation with the deuteron- stripping. Indeed, such an effect is well known for (d, p) reactions, for which a significant increase of the cross section, connected with the polarization of the weakly bound deuteron, is observed below the barrier (the so called Oppenheimer-Phillips resonance [27]). In our case, this effect may be stronger because of the smaller neutron binding energy in ^{6}He compared to that for the deuteron and the larger repulsive forces of the α-particle compared to the proton. Additionally, it has been speculated in [28] that the observed enhanced ^{6}He total reaction cross section is due to the quite probable dipole excitation. This excitation occurs because the two halo neutrons are well separated from the charged core and the centers of charge and mass of the ^{6}He nucleus do not coincide. For energies close to the Coulomb barrier dipole excitation can predominate as a result of the long-range Coulomb forces, which in turn leads to deformation and breakup of ^{6}He [29]. In both cases, neutrons can be transferred to the target nucleus. Also, the large formation cross section for ^{198}Au could be the result of the interaction of a quasi-free neutron in ^{6}He with the ^{197}Au target.

Meanwhile it seems, the increased formation probability of reaction products at energies close to the barrier, which imitate the transfer of one neutron to the target nucleus, can be used to explain the formerly observed in [6,7] enhanced probability of sub-barrier fission in the ^{238}U + ^{6}He reaction.

The isotope ^{196}Au. The cross section for pick-up from ^{197}Au smoothly decreases in the direction of the Coulomb barrier and then at a value of about

10 mb gets saturated, and after that falls down again until the value of the 1n-transfer reaction threshold of ~8.5 MeV is reached. This behaviour can be explained by different mechanisms of formation of the ^{196}Au isotope (-1n channel). At energies well above the Coulomb barrier, it seems that predominantly knock-out of a neutron from the target occurs. At energies close to and below the Coulomb barrier, several contributions to the formation of ^{196}Au are possible. One is due to the evaporation of one neutron after an inelastic process on ^{197}Au (excited ^{197}Au* nuclei are produced). ^{196}Au can be produced after the evaporation of three neutrons from ^{199}Au, if the latter were excited to E* ≈ 27-36 MeV. Additionally, the recoil nucleus ^{198}Au, produced in the 1n-transfer channel, can be excited to E* ≈ 18-32 MeV so that it can decay to ^{196}Au by the emission of two neutrons. These processes can explain, at least partially, the flat shape of the excitation function, observed in the region E_{lab} ≈ 12-28 MeV. The nucleus ^{196}Au itself can decay by emission of neutrons only at E* > 8 MeV, which can be reached at incident energies higher than 16-18 MeV.

The isotopes ^{194}Au and ^{195}Au. As we can see from Table 2 the isotope ^{195}Au has characteristics that are not convenient for its detection. It has a very long (~186 days) half-life and its most intensive γ-rays is in the region of energies, where we observed significant background. The isotope ^{194}Au was observed at the highest in our case beam energies (~50-60 MeV) and as is shown in Fig. 8, its formation cross section amounts to ~30 mb, but quickly decreases at lower energies and at 48.5 MeV we got an upper limit of 8.4 mb.

The cross sections for the different reaction channels (fusion and transfer) of ^{6}He are presented in Fig. 9, as a function of the difference E_{cm} - B_c. The excitation function for the fusion of ^{4}He with ^{197}Au is also shown for comparison. One can see the increase in the cross section for the ^{6}He + ^{197}Au fusion reaction in the sub-barrier region compared to the case of ^{4}He, and also the rather strong increase of the formation cross section of ^{198}Au.

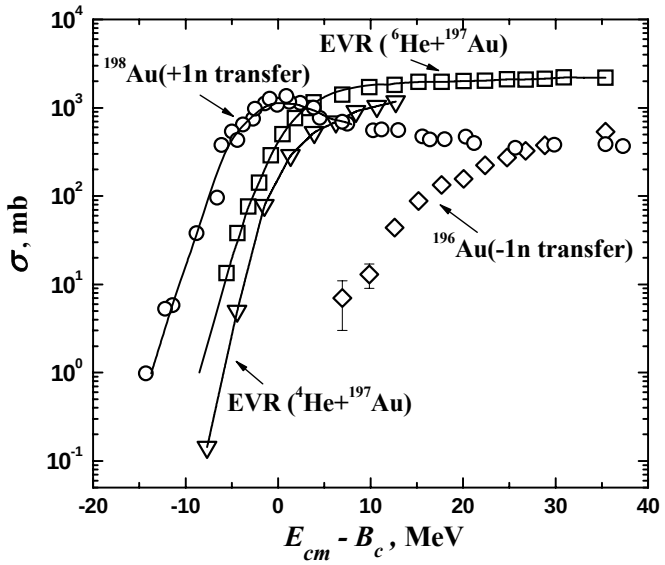

Fig. 9. Experimental cross sections for complete fusion (∀), for formation of ^{196}Au (M) and ^{198}Au (–) in the reaction ^{6}He + ^{197}Au (present experiment), and for complete fusion (X) in the ^{4}He + ^{197}Au reaction [23] as a function of the difference between the center of mass energy and the Coulomb barrier ($E_{см}$ - B_c). The curves are drawn to guide the eye.

CONCLUSIONS

In the present paper, we have presented results on the measurements of the excitation functions for fusion and transfer products in ^{6}He induced reactions on ^{197}Au and ^{206}Pb in a wide energy range including deep sub-barrier energies. The experiments were performed at the accelerator complex DRIBs in Dubna, the ^{6}He beam intensity reaching $2 \cdot 10^{7}$ pps at 10 MeV/A.

The following conclusions can be drawn. The data on fusion reactions, followed by the evaporation of two neutrons (^{206}Pb+^{6}He and ^{197}Au+^{6}He) at energies close to the Coulomb barrier differ from predictions within the framework of the statistical model for compound nuclei decay. For these exit channels a strong enhancement is observed and this is in agreement with the model of "sequential fusion" [24]. The reactions of transfer of one neutron from ^{6}He to the ^{197}Au target nucleus at deep sub-barrier energies (B_{cm} - E_{cm} <

15 MeV) take place with relatively high probability. This may be connected with the interaction of quasi-free neutrons.

Finally, the authors would like to express their gratitude to the accelerator staff for the great effort to put into operation the accelerator complex DRIBs and to obtain the ^{6}He beam. We are also indebted to M.G. Itkis and S.N. Dmitriev for their support, and to V.I. Zagrebaev for making available his calculations of the fusion reaction cross sections and for fruitful discussions. Thanks are due also to D.N. Rassadov, S.V. Shishkin and J. Adam for their help during the performance of the experiments.

The present investigation was carried out with the support of RFFR by grant № 04-02-17372, as well as by grants from the Czech Republic, Poland and Bulgaria in the frame of their collaboration with JINR.

REFERENCES

1. *Penionzhkevich Yu.E. et al.* // Nucl. Phys. A. 1995. V. 588. P. 258; *Fomichev A.S. et al.* // Z. Phys. A. 1995. V. 351. P. 129.
2. *Hussein M.S. et al.* // Phys. Rev. C. 1992. V. 46. P. 377; Nucl. Phys. A. 1995. V. 588. P. 85c.
3. *Dasso C. et al.* // Nucl. Phys. A. 1996. V. 597. P. 473.
4. *Stelson P.H.* // Phys. Rev. C. 1990. V. 41. P. 1584.
5. *Kolata J.J. et al.* // Phys. Rev. Lett. 1998, V. 81, N. 21, P. 4580.
6. *Trotta M. et al.* // Phys. Rev. Lett. 2000, V. 84, N. 11, P. 2342.
7. *Raabe R., Sida J.L., Trotta M. et al.* // Nature, 2004, V. 431, P. 823.
8. *Di Pietro A. et al.* // Phys. Rev. C. 2004. V. 69. P. 044613.
9. *Navin A. et al.* // Phys. Rev. C. 2004. V. 70. P. 044601.
10. *Oganessian Yu.Ts. and Gulbekian G.G.* // In: Proc. of the Int. Conf. "Nuclear Shells - 50 Years", Dubna, Russia, 1999, Eds. Oganessian Yu.Ts., von Oertzen W. and Kalpakchieva R. (World Scientific, Singapore, 2000) p. 61.
11. *Penionzhkevich Yu.E. et al.* // Preprint JINR E7-2005-106, Dubna 2005.
12. *Kuznetsov V.D. et al.* // Scientific report FLNR 2001-2002, P. 223 and 224, Ed. Popeko A.G., JINR, Dubna, 2003.

13. *Astabatyan R.A. et al.* // Scientific report FLNR 2001-2002, P. 212, Ed. Popeko A.G., JINR, Dubna, 2003. Scientific report FLNR 2003-2004, Ed. Popeko A.G., JINR, Dubna, 2005.
14. *Skobelev N.K. et al.* // Nucl. Instr. Meth. B. 2005. V. 227. P. 471.
15. http://dnr080.jinr.ru/lise/
16. *Frana J.* Program Deimos 32 for Gamma-Ray Spectra Evaluation // Radioanal. and Nucl. Chem. 2003. V. 257. P. 583.
17. http://nucleardata.nuclear.lu.se/NuclearData/toi/
18. *Gritchenko Z.G. et al*. // Physics of Atomic Nuclei. 1969. V. 10. P. 929 (In Russian).
19. Experimental Nuclear Physics, Ed. E.Segrè, New York-London, 1959, V.3, Part 8.
20. *Muzychka Yu.A. and Pustylnik B.I.* // Physics of Atomic Nuclei. 1987. V. 45. P. 90.
21. *Penionzhkevich et al.* // Physics of Atomic Nuclei, V. 65, no. 9. 2002. P. 1563.
22. *Lanzafame F.M. and Blann M.* // Nucl. Phys. A. 1970. V. 142. P. 545.
23. *Kulko A.A. et al.* // Preprint JINR R7-2006-14, Dubna 2006 (in Russian).
24. *Zagrebaev V.I.* // Phys. Rev. C. 2003. V. 67. P. 061601(R); Progr. Theor. Phys. Suppl. 2004. V.154. P. 122.
25. *Bimbot R. et al.* // Nucl. Phys. A. 1972. V. 189. P. 193.
26. *Audi G. et al.* // Nucl. Phys. A. 2003. V. 729. P. 337.
27. *Oppenheimer J.R. and Phillips M.* // Phys. Rev. 1935. V. 48. P. 500.
28. *Keeley N. et al.* // Phys. Rev. C. 2003.V. 68. P. 054601.
29. *Dasso C. H. et al.* // In: Proc. 2nd Japan-Italy Joint Symposium'95 (Riken, Japan, May 1995) "Perspective in Heavy Ion Physics" Word Scientific, Singapore, 1996, P. 42.

Отпечатано методом прямого репродуцирования с оригинала,
предоставленного авторами.

Подписано в печать 26.05.2006.
Формат 60 × 90/16. Бумага офсетная. Печать офсетная.
Усл. печ. л. 1,43. Уч.-изд. л. 2,05. Тираж 350 экз. Заказ № 55354.

Издательский отдел Объединенного института ядерных исследований
141980, г. Дубна, Московская обл., ул. Жолио-Кюри, 6.
E-mail: publish@pds.jinr.ru
www.jinr.ru/publish/